Studies on the Interaction of THF with FER Zeolite

De-Chang Lin,[†,‡] Wei-Zheng Zhou,[†] Juan Guo,[†] He-Yong He,[†] and Ying-Cai Long*[,†]

Laboratory of Molecular Catalysis and Innovative Materials, Department of Chemistry, Fudan University, Shanghai 200433, P. R. of China, and School of Pharmacy, Second Military Medical University, Shanghai 200433, P. R. of China

Received: August 14, 2002; In Final Form: January 30, 2003

The interaction of tetrahydrofuran (THF), a template, with FER type zeolite was studied by molecular simulation and ^{13}C high-power decoupling magic angle spinning nuclear magnetic resonance (HPDEC MAS NMR) spectrometry. Molecular dynamics (MD) together with energy minimization (EM) methods were used to simulate the interactions of Si−FER with THF, and with two other templates of pyrrolidine and pyridine for comparison. The interaction energies for these templates located in FER ($8^2 6^2 6^4 5^8$) cage and in the 10 member ring (MR) channel were calculated, respectively. The preferred binding site for each template investigated is the FER cage site. The variation of the calculated potential energy indicates a high-energy barrier for the moving of THF molecule to the 10-MR channel from FER cage. The experiments of ^{13}C HPDEC MAS NMR demonstrate that the molecules of THF are located in FER cages as the template, and in the 10-MR channels as the adsorbed molecules.

Introduction

Studies on the templating effect of some organic species are greatly important and interesting.[1−4] This is because using these organics as the structure-directing agent or template can introduce the formation of novel structures, increase the Si/Al ratio of the framework, and promote the crystallization in the synthesis process of zeolite molecular sieves.

Some experimental techniques, such as XRD structural determination of single crystal, NMR, powder XRD, FT-IR, TG/DTG/DTA, etc., have been employed to investigate the structural details of the template within zeolite.[5−7] The most important and useful method among these techniques should be single crystal XRD structure analysis. Because of the difficulty of growing large single crystals of zeolite, the molecular simulation technique has been widely used as a powerful tool to obtain the useful information of the template trapped in zeolite.[8−13]

The molecular simulation technique shows an increasing importance in zeolite science. The technique helps us to understand the role of the template in the process of the nucleation and the growth for zeolite crystallization. It would be possible to predict the templating ability of several assumed template agents by simulation and then select a suitable one or more as the template for inducing the formation of a given zeolite framework. Lewis et al.[14] have rationalized the templating ability in terms of energetic. They found a reasonably good correlation between the nonbonding energy and the number of non-hydrogen atoms in the template molecule. A number of other works of the rationalization for zeolite synthesis are available based on the computer simulation reported in the literature.[15−17]

MD, Monte Carlo (MC), and EM[6,11−13,18−24] are three major simulation methods in searching the binding site for template or adsorbate in zeolites. These methods are often used in combining with each other or with the simulated annealing technique.[11−13,19,23] Usually, the EM calculation presents the local minimum conformer but not global minimum conformer as the result. Then different starting conformers have to be tried.[25]

FER type zeolite (ferrierite, ZSM-35, FU-9, and NU-23) has been found to be an excellent shape-selective catalyst for skeletal isomerization of *n*-alkenes to isoalkenes, especially for *n*-butene to isobutene.[26−29] The zeolite possesses orthorhombic framework. In the cell, there are two 10-MR straight channels with size 4.2 × 5.4 Å, two 6-MR straight channels parallel [001], and two 8-MR straight channels with size 3.5 × 4.8 Å parallel [010]. A spherical cavity with a size of 6∠7 Å called the ($8^2 6^2 6^4 5^8$) cage or FER cage forms by an intersection of the 8-MR and 6-MR channel. Many studies on the synthesis and the characterization of the zeolite have been reported.[30−43] More than 30 organic compounds such as pyridine,[30,31] pyrrolidine,[34,39,40] ethylenediamine,[41] glycerol,[42] etc., have been employed as the template. In our group a novel method for synthesis of FER zeolite has been developed using THF (tetrohydrofuran), a nitrogen free organic compound, as the template.[44,45] The crystallization of FER, MTN, MFI, and MOR zeolite with THF as the template was investigated.[7,46]

In this work, the interaction of FER type zeolite framework with the template molecules of THF, pyridine, and pyrrolidine, which possess similar molecular configurations and sizes, is investigated by simulation. The simulation result of THF/FER is in good agreement with the deduction obtained from the experiments of ^{13}C high-power decoupling magic angle spinning nuclear magnetic resonance (HPDEC MAS NMR) and adsorption. The result of pyridine/FER is compared with the work of Weigel et al.[32] As far as we know, no other simulation result of pyrrolidine/FER was reported.

Experimental Section

Sample Preparation. Sample A, Na−THF−FER zeolite, was hydrothermally synthesized according to our previous work.[44]

* To whom correspondence should be addressed. Email: yclong@fudan.edu.cn.
† Fudan University.
‡ Second Military Medical University.

10.1021/jp026756x CCC: $25.00
Published on Web 04/01/2003

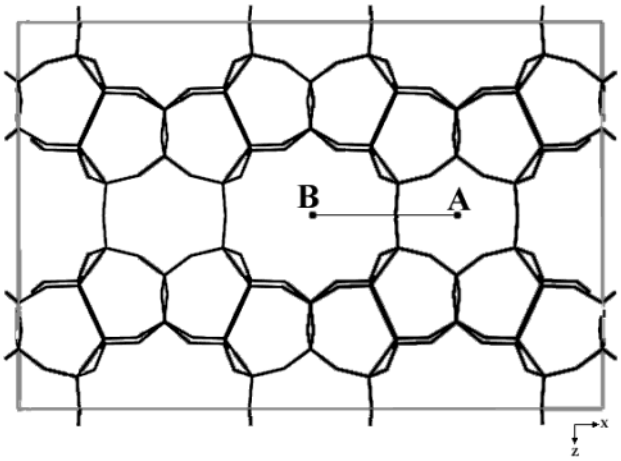

Figure 1. Moving pathway from the FER cage to the 10-MR channel for the THF molecule.

The molar composition of the reactant gel was 0.5 THF:0.215 Na_2O:1.0 SiO_2:0.05 Al_2O_3:20 H_2O with silica sol and aqueous solution of aluminum sulfate as the raw materials. The reactant gel was sealed into a 30 mL stainless steel autoclave and crystallized in an oven at 200 °C for 8−12 days under static conditions. The crystallized product was washed with distilled water, filtered and dried at 100 °C.

Sample B, H−THF−FER, was prepared by ion exchange of sampele A with 0.5 mol·L^{-1} HCl aqueous solution under stirring at ambient temperature for 4 h. After ion exchange, the sample was washed with distilled water, filtered, and dried at 100 °C.

Sample C, Na−FER/THF, was obtained by the adsorption of THF in a vacuum at 20 °C on the sample of Na−FER, which was prepared by calcination of sample A at 550 °C for 6 h for removing the template of THF in the as-synthesized zeolite.

Sample D, H−FER/THF, was obtained by the adsorption of THF in a vacuum at 20 °C on the sample of H−FER, which was prepared by calcination of sample B at 550 °C for 6 h for removing the template of THF in the ion-exchanged sample.

Characterization. Powder XRD was carried out with a Rigaku D-MAX/IIA X-ray powder diffractometer. Cu Kα radiation ($\lambda = 1.5418$ Å) was used. TG/DTG/DTA analysis was carried out on a Rigaku PTC-10A thermal analyzer. About a 10 mg sample of the investigated FER zeolite was used for each measurement. The temperature rose from room temperature to 900 °C at a rate of 10 °C·min^{-1} in a flow of air. The ^{13}C HPDEC MAS NMR spectra of the samples were collected at room temperature on a Bruker DSX-300 spectrometer. The resonance frequency used was 75.467 MHz. The radio frequency field was 50 kHz. The rotor was spun at 3.5 kHz, a 2k FID was required, corresponding to a $\pi/2$ pulse width of 5 μs. A recycle time of 3 s and a delay time of 6 μs were used with a spectral width of 21 097.047 Hz. Adamantane was used as a second reference, whose higher field resonance peak has a chemical shift of $\delta = 38.83$ with respect to TMS (tetramethylsilane) as zero.

The contents of Si and Al of the samples were measured by using energy dispersion X-ray analysis (EDX) on a Philips XL 30 scanning electron microscope at 20 kV. The content of Na was determined by an inductively coupled plasma (ICP) atomic emission spectrometer. The content of THF in Na−THF−FER and H−THF−FER was calculated by the weight loss in the TG curves at >300 °C.

The identification with XRD (Figure 1S, see Supporting Information) confirms that the as-synthesized Na−THF−FER zeolite is a pure phase with high crystallinity. The cell compositions calculated from the data of the determined contents are $Na_{2.80}Al_{2.91}Si_{33.09}O_{72}$·1.50THF and $H_{2.64}Na_{0.16}Al_{2.80}Si_{33.20}O_{72}$·1.45THF for the sample of the as-synthesized Na−THF−FER and H−THF−FER, respectively. The result shows that Na^+ in the as-synthesized zeolite is much easily exchanged with H^+ in mild condition, and THF molecule keeps in the channels of the zeolite in the process of ion-exchange.

Modeling and Computational Details. The cell parameters of $a = 14.07025$ Å, $b = 7.41971$ Å, $c = 18.720$ Å, $\alpha = \beta = \gamma = 90°$ and the atom coordinates of the Si−FER zeolite structure with *Pnnm* space group were taken from ref 47. There are four unit cells ($2 \times 2 \times 1$) in the simulation box, and the periodic boundary conditions are applied to simulate an infinite system. The template molecules investigated are flexible, whereas the zeolite framework geometry is fixed.

The models were built with a Visualizer module, the molecular dynamics and the minimization calculations were performed on the Discover module of Materials Studio (Version 1.2) software available from Molecular Simulation Inc. (MSI, and now is Accelrys).[25] Polymer Consistent Force Field (PCFF) was employed. The MD simulations were performed within a canonical ensemble (NVT) at 773 K, and the temperature was controlled by Andersen method. The atom-based summation technique was employed to calculate the nonbonded interactions (van der Waals and electrostatic), with a cutoff radius of 15 Å. The total simulation time is 5×10^5 fs (500 ps), and the time step is 1 fs. The trajectory information was recorded every 20 fs. The first 1000 records (20 000 fs) were neglected when the trajectory file was analyzed. The conformer with lowest energy was minimized using the cell-based summation method to compute the nonbonded interactions. The smart minimizer was employed, combining the steepest descents method and conjugate gradient method.

E_{total}, the potential energy of a system can be expressed as a sum of valence ($E_{valence}$), crossterm ($E_{crossterm}$), and nonbonded ($E_{nonbond}$) interaction:[25]

$$E_{total} = E_{valence} + E_{crossterm} + E_{nonbond}$$

The sum of first the two terms, $E_{valence}$ and $E_{crossterm}$, are reported as internal potential ($E_{internal}$) in the output file. The last term, $E_{nonbond}$, includes van der Waals (vdW) interaction and electrostatic (coulomb) interaction.

$E_{interact}$, the interaction energy of guest/host (template/zeolite), or E_{bind}, the binding energy, can be calculated as the following formula:

$$E_{interact} = -E_{bind} = E_{zeo-mol} - E_{zeo} - E_{mol}$$

where E_{zeo}, E_{mol} is the potential energy of the zeolite framework and the template molecule, respectively. $E_{zeo-mol}$ is the total potential energy of the zeolite/template system.

We assumed that a pathway exists between site A, the binding site in the FER cage, and site B, the adjacent binding site in the 10-MR channel (Figure 1). The center-of-mass for the template molecule is plotted as a spot. The distance between site A and site B is about 7 Å. Starting from site A, the THF molecule translates and moves toward site B along the pathway. The path is divided into several small steps with each distance of 0.5 Å. The interaction energy of the THF molecule in the FER framework was calculated for all conformations after the local minimum was searched through the energy minimization with the center-of-mass of the THF molecule being constrained.

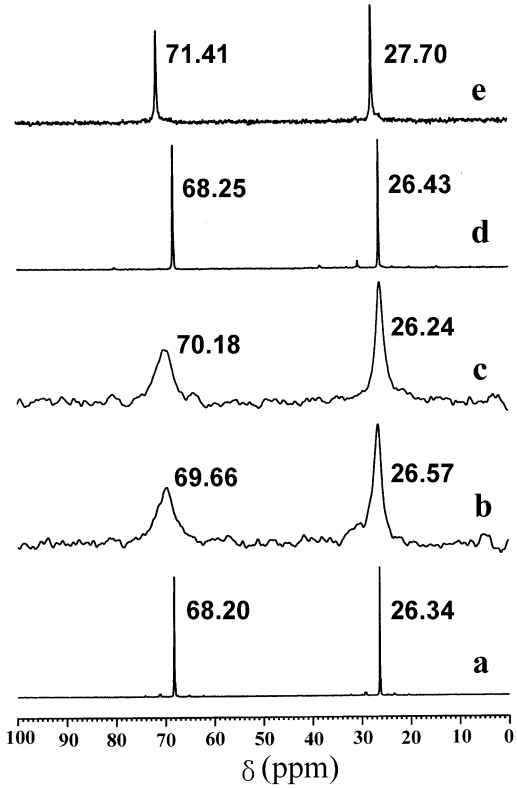

Figure 2. ^{13}C HPDEC MAS NMR spectra of THF: (a) in the liquid phase; (b) in sample A, Na−THF−FER; (c) in sample B, H−THF−FER; (d) in sample C, H−FER/THF; (e) in sample D, Na−FER/THF.

TABLE 1: ^{13}C HPDEC MAS NMR Data for THF in the Samples

	C(1)[a]		C(2)[b]	
samples	δ (ppm)	ΔH (Hz)[c]	δ (ppm)	ΔH (Hz)
THF	68.20	2	26.34	1
Na−THF−FER	69.66	230	26.57	80
H−THF−FER	70.18	250	26.24	80
Na−FER/THF	68.25	9	26.43	9
H−FER/THF	71.41	14	27.70	10

[a] C(1): $-CH_2-\boldsymbol{C}H_2-O-$. [b] C(2):$-CH_2-\boldsymbol{C}H_2-CH_2-$. [c] ΔH: full width of half-maximum (fwhm).

Results and Discussion

NMR Experiments. ^{13}C HPDEC MAS NMR spectra of THF in FER zeolite samples are shown in Figure 2. Table 1 lists the data of the ^{13}C HPDEC NMR spectrum of each investigated sample.

It can be deduced that the molecules of THF are located in FER cages, in which the rotation of THF molecules is restricted, leading to the ^{13}C resonance peak of THF being broadened in Na−THF−FER and H−THF−FER (Figure 2b,c and Table 1). On the other hand, the chemical shifts of THF are respectively at 70.18 ppm (C1) and 26.24 ppm (C2) in H−THF−FER and at 69.66 ppm (C1) and 26.57 ppm (C2) in Na−THF−FER, respectively, showing almost the same values of chemical shift. The fact that these are almost the same chemical shift values indicates that the influence of the ions (Na^+, H^+) in the FER zeolite on the chemical shift of THF is very weak, and the molecules of THF still remain in FER cages whereas Na^+ ions are exchanged with H^+ ions.

The resonance peaks of THF in the spectra of Na−FER/THF and H−FER/THF are very narrow in comparison with the peaks in the spectra of H−THF−FER and Na−THF−FER, showing that the rotation of THF molecules is quite free in the zeolite. The δ_{C1} of THF adsorbed in H−FER obviously moves to **a** lower field than that of THF adsorbed in Na−FER. The resonance peaks of THF in H−FER are slightly broader than that in Na−FER. It shows that the interaction of THF molecules with H^+ ion is stronger than that with the Na^+ ion. Obviously, these data for the adsorbed molecules of THF are different from those of THF in the sample of H−THF−FER and Na−THF−FER, indicating various chemical environments and different interactions with the framework for THF in these samples. Therefore, we can deduce that the adsorbed THF molecules are located in the 10-MR channels of H−FER zeolite and Na−FER zeolite. On the other hand, the template molecules of THF are trapped in FER cages of the as-synthesized Na−THF−FER zeolite and H−THF−FER zeolite.

TABLE 2: Binding Energy for Template Molecules in Si−FER Zeolite (kJ·mol^{-1})

	present results		results reported[a]	
template	FER cage	10-MR channel	FER cage	10-MR channel
THF (C_4H_8O)	77.66 (15.53)[b]	58.98 (11.80)		
pyrrolidine (C_4H_9N)	68.26 (13.65)	56.34 (11.27)		
pyridine (C_5H_5N)	78.21 (13.03)	65.38 (10.90)	78	62

[a] Reference 32. [b] The values in parentheses present the binding energy per non-hydrogen atom.

Interaction of Template and Si−FER Zeolite. Figure 3 shows the conformer of the molecules of THF, pyrrolidine, and pyridine in the framework of a Si−FER zeolite. The primary plane of each investigated template molecule is parallel to [001] in the 10-MR channel and almost parallel to [010] in the FER cage. The calculated binding energies for pyridine in FER zeolite are quite similar with that obtained by Weigel et al.[32] (Table 2). The orientations of pyridine molecules in the conformers are almost the same as those reported in Weigel et al.'s paper,[32] and we also found that the pyridine molecules tilt within the FER-cage when compared to the framework topology (Figure 3S).

Table 2 lists the data of E_{bind}, the binding energy for THF, pyridine, and pyrrolidine in Si−FER, respectively. The binding energy in the Si−FER-cage site is higher than that of in the 10-MR channel site for each template, indicting that the molecules of these templates prefer the cage site. The difference of the binding energy in the two sites for THF (18.68kJ·mol^{-1}) was higher than that for pyridine (12.83 kJ·mol^{-1}) and pyrrolidine (11.92 kJ·mol^{-1}).

The simulation results indicate that the order of the templating ability of these investigated organic molecules for Si−FER structure is pyridine > THF > pyrrolidine according to E_{bind}. Because the molecule of pyridine possesses more non-hydrogen atoms, the templating ability order should actually be THF > pyrrolidine > pyridine when the binding energy per non-hydrogen atom is considered.

Energy Barrier. Figure 4 shows the curve of the interaction energy vs the distance between the center-of-mass for THF molecule and the starting position of site A. The interaction energy increases at first while the THF molecule moves from A toward B and then reaches the maximum (about 178.6 kJ·mol^{-1} at the distance of ~3.5 Å from position A) when the molecule passes through the 8-MR window. A descent of the interaction energy follows after the molecule enters the 10-MR channel. The high-energy barrier of 256.3 kJ·mol^{-1} makes it

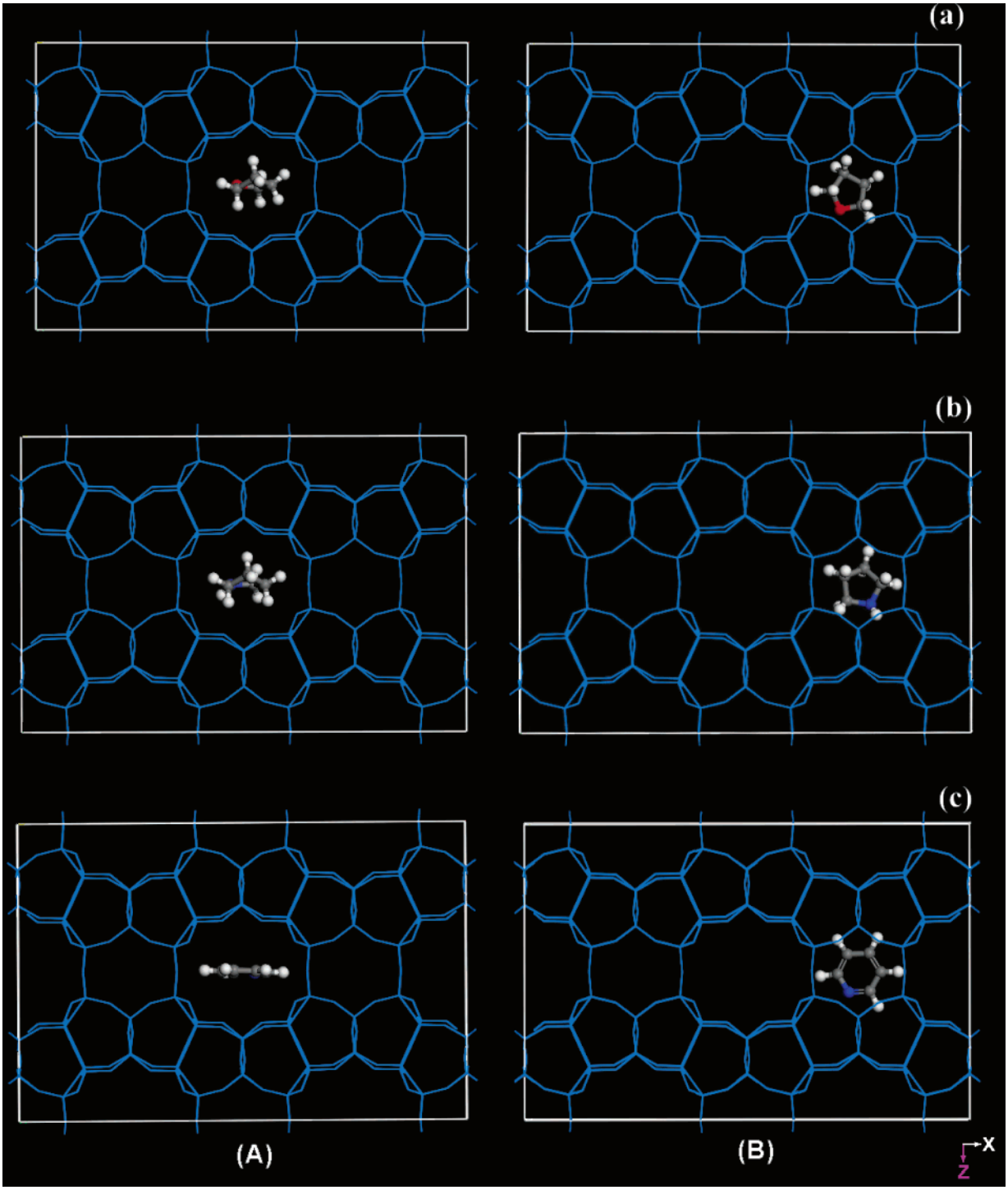

Figure 3. Simulated binding positions of THF (a), pyrrolidine (b), and pyridine (c) in Si−FER zeolite framework viewed down [010] direction: (A) in the 10-MR channel; (B) in the FER cavity.

impossible for THF molecule crossing the 8-MR windows in normal condition, except under high temperature. This result is consistent with the fact that THF molecules remain in the FER cavity whereas the as-synthesized zeolite was exchanged with H^+ at ambient temperature, and the absorbed THF molecules can only occupy the 10-MR channels. In a realistic system, the zeolite framework is flexible, which may be beneficial to THF molecules for passing through the 8-MR windows. Obviously, the van der Waals repulsive interaction and the internal potential energy, in which the former is the major, contribute to the energy barrier. The change of the electrostatic interaction is little in comparison with that of other two terms.

Conclusions

The interactions of THF with FER zeolite were studied by molecular simulation and ^{13}C HPDEC MAS NMR experiments in this work. Combining the method of molecular dynamics and energy minimization, the interactions of Si−FER zeolite with THF and two other templates, pyrrolidine and pyridine, were investigated. The preferred site for each template in the zeolite framework is the cage site. The primary plane of these molecules is almost parallel to [010] when they are located in the cage, and parallel to [001] when in the 10-MR channel. The calculated interaction energies of these templates and FER zeolite are at

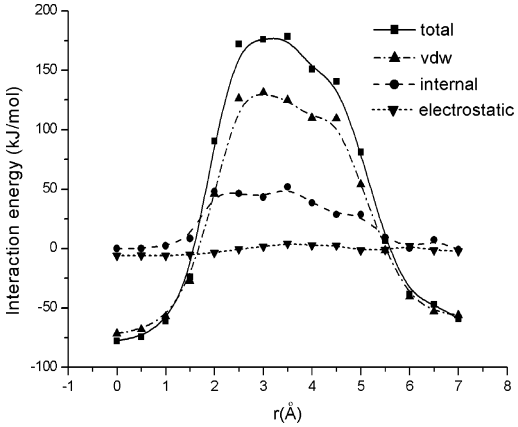

Figure 4. Interaction energy for THF in FER as a function of the distance from the cage binding site.

the same level. The templating ability order for the FER structure is THF > pyrrolidine > pyridine according to the interaction energy per non-hydrogen atom.

Relatively, the difference of the interaction energy in the FER-cage and in the 10-MR channel for THF is more than that for pyridine and pyrrolidine. It indicates that the opportunity of occupying the cage site is much more than that in the 10-MR channel for THF. The molecules of THF as well as pyridine or pyrrolidine cannot pass through the 8-MR windows, due to the van der Waals repulsive potential increasing rapidly while the template molecules cross the 8-MR windows.

^{13}C HPDEC MAS NMR spectra and the adsorption experiment give evidence that THF molecules are trapped in the FER cage in the as-synthesized Na−THF−FER and ion-exchanged H−THF−FER, whereas THF molecules are adsorbed in the 10-MR channels of Na−FER and H−FER. These results strongly support the deduction from the molecular simulation.

Acknowledgment. This work is supported by the National Natural Science Foundation of China (Projects 20073010 and 20005310). Figures 1 and 3 were generated by using Materials Studio.

Supporting Information Available: Three additional figures displaying (a) in situ X-ray powder diffraction pattern of FER samples, (b) the TG/DTA/DTG curves, and (c) the pyridine molecule tilted in the FER cage. This material is available free of charge via the Internet at http://pubs.acs.org.

References and Notes

(1) Gies, H.; Marler, B. *Zeolites* **1992**, *12*, 42.
(2) Rollmann, L. D.; Schlenker, J. L.; Lawton, S. L.; Kennedy, C. L.; Kennedy, G. J.; Doren, D. J. *J. Phys. Chem. B* **1999**, *103*, 7175.
(3) Rollmann, L. D.; Schlenker, J. L.; Kennedy, C. L.; Kennedy, G. J.; Doren, D. J. *J. Phys. Chem. B* **2000**, *104*, 721.
(4) Li, J.; Yu, J.; Yan, W.; Xu, Y.; Qiu, S.; Xu, R. *Chem. Mater.* **1999**, *11*, 2600.
(5) Lewis, J. E.; Freyhardt, C. C.; Davis, M. E. *J. Phys. Chem.* **1996**, *100*, 5039.
(6) Loiseau, T.; Mellot-Draznieks C.; Sassoye C.; Sassoye, C.; Girard, S.; Guillou, N.; Huguenard, C.; Taulelle, F.; Ferey, G. *J. Am. Chem. Soc.* **2001**, *123*, 9642.
(7) Qian, B.; Guo, G.; Wang, X.; Zeng, Y.; Sun, Y.; Long, Y. *Phys. Chem. Chem. Phys.* **2001**, *3*, 4164.
(8) Sabater, M. J.; Sastre, G. *Chem. Mater.* **2001**, *13*, 4520.
(9) Chatterjee, A. *J. Mol. Catal. A*: *Chem.* **1997**, *120*, 155.
(10) Chatterjee, A.; Vetrivel, R. *J. Mol. Catal. A: Chem.* **1996**, *106*, 75.
(11) Boyett, R. E.; Stevens, A. P.; Ford, M. G.; Cox, P. A. *Zeolites* **1996**, *17*, 508.
(12) Wright, P. A.; Maple, M. J.; Slawin, A. M. Z.; Patinec, V.; Aitken, R. A.; Welsh, S.; Cox, P. A. *J. Chem. Soc., Dalton Trans.* **2000**, *8*, 1243.
(13) Patinec, V.; Wright, P. A.; Aitken, R. A.; Lightfoot, P.; Purdie, S. D. J.; Cox, P. A.; Kvick, A.; Vaughan, G. *Chem. Mater.* **1999**, *11*, 2456.
(14) Lewis, D. W.; Freeman, C. M.; Catlow, C. R. A. *J. Phys. Chem.* **1995**, *99*, 11194.
(15) Yu, J.; Li, J.; Wang, K.; Xu, R.; Sugiyama, K.; Terasaki, O. *Chem. Mater.* **2000**, *12*, 3783.
(16) Zhou, B.; Yu, J.; Li J.; Xu, Y.; Xu, W.; Qiu, S.; Xu, R. *Chem. Mater.* **1999**, *11*, 1094.
(17) Wang, L.-J.; Li, B.-H.; Chen, T.-H.; Jin, Q.-H.; Wang, J.-Z.; Tang, S.-X.; Ding, D.-T. *Chin. J. Inorg. Chem.* **2000**, *16*, 739.
(18) Haase, F.; Sauer, J. *Micropor. Mesopor. Mater.* **2000**, *35*−*36*, 379.
(19) Domokos, L.; Lefferts, L.; Seshan, K.; Lercher, A. *J. Catal.* **2001**, *203*, 351.
(20) Smit, B.; Siepmann, J. I. *J. Phys. Chem.* **1994**, *98*, 8442.
(21) Jousse, F.; Auerbach, S. M.; Vercauteren, D. P. *J. Phys. Chem. B* **2000**, *104*, 2360.
(22) Titiloye, J. O.; Parker, S. C.; Stone, F. S. *J. Phys. Chem.* **1991**, *95*, 4038.
(23) Nascimento, M. A. C. *J. Mol. Struct. (THEOCHEM)* **1999**, *464*, 239.
(24) Hou, T. J.; Zhu, L. L.; Li, Y. Y.; Xu, X. J. *J. Mol. Struct. (THEOCHEM)* **2001**, *535*, 9.
(25) Materials Studio. V.1.2. 2001, Accelrys.
(26) Pirngruber, G. D.; Zinck-Stagno, O. P. E.; Seshan, K.; Lercher, J. A. *J. Catal.* **2000**, *190*, 374.
(27) Xu, W.-Q.; Yin, Y.-G.; Suib, S. L.; Edwards, J. C.; O'Young, C.-L. *J. Phys. Chem.* **1995**, *99*, 9443.
(28) Pieterse, J. A. Z.; Seshan, K.; Lercher, J. A. *J. Catal.* **2000**, *195*, 326.
(29) Guisnet, M.; Andy, P.; Gnep, N. S.; Benazzi, E.; Travers, C. *J. Catal.* **1996**, *158*, 551.
(30) Kuperman, A.; Nadimi, S.; Oliver, S.; Ozin, G. A.; Garces, J. M.; Olken, M. M. *Nature* **1993**, *365*, 239.
(31) Morris, R. E.; Weigel, S. J.; Henson, N. J.; Bull, L. M.; Janicke, M. T.; Chmelka, B. F.; Cheetham, A. K. *J. Am. Chem. Soc.* **1994**, *116*, 11849.
(32) Weigel, S. J.; Gabriel, J.-C.; Puebla, E. G.; Bravo, A. M.; Henson, N. J.; Bull, L. M.; Cheetham, A. K. *J. Am. Chem. Soc.* **1996**, *118*, 2427.
(33) Zholobenko, V. L.; Lukyanov, D. B.; Dwyer, J.; Smith, W. J. *J. Phys. Chem. B* **1998**, *102*, 2715.
(34) Jacob, N. E.; Joshi, P. N.; Shaikh, A. A.; Shiralkar, V. P. *Zeolites* **1993**, *13*, 430.
(35) Khomane, R. B.; Kulkarni B. D.; Ahedi, R. K. *J. Colloid Interface Sci.* **2001**, *236*, 208.
(36) Shevade, S. S.; Rao, B. S. *Catal. Lett.* **2000**, *66*, 99.
(37) Pieterse, J. A. Z.; Veefkind-Reyes, S.; Seshan, K.; Lercher, J. A. *J. Phys. Chem. B* **2000**, *104*, 5715.
(38) Onyestyak, G.; Pal-Borbely, G.; Rees, L. V. C. *Micropor. Mesopor. Mater.* **2001**, *43*, 73.
(39) Shevade, S.; Ahedi, R. K.; Kotasthane, A. N. *Catal. Lett.* **1997**, *49*, 69.
(40) Ahedi, R. K.; Kotasthane, A. N.; Rao, B. S.; Manna, A.; Kulkarni, B. D. *J. Colloid Interface Sci.* **2001**, *236*, 47.
(41) Li, J.; Liu, G.; Li, J. *Catal. Lett.* **1993**, *20*, 345.
(42) Kanno, N.; Miyake, M.; Sato, M. *Zeolites* **1994**, *14*, 625.
(43) Forbes, N. R.; Rees, L. V. C. *Zeolites* **1995**, *15*, 444.
(44) Guo, G.-Q.; Sun, Y.-J.; Long, Y.-C. *Chem. Commun.* **2000**, 1893.
(45) Long, Y. C.; Guo, G. Q. *Chin. Pat.* **2000**, 00 111 893.
(46) Qian, B.; Jiang, H.-W.; Sun, Y.-J.; Long, Y.-C. *Langmuir* **2001**, *17*, 1119.
(47) Treacy, M. M. J.; Higgins, J. B.; von Ballmoos, R. *Collection of Simulated XRD Powder Patterns for Zeolites*, 3rd revised ed.; Elsevier: New York, 1996; p 710.